Supporting Information

Shell Thickness Effects on Quantum Dot Brightness and Energy Transfer

Margaret Chern,[a] Thuy T. Nguyen,[b] Andrew H. Mahler,[b] Allison M. Dennis[b,*]
[a] Division of Materials Science and Engineering, Boston University
[b] Department of Biomedical Engineering, Boston University
Boston, Massachusetts, 02446, USA
* corresponding author: Allison M. Dennis, aldennis@bu.edu

1. QD Characterization

1.1 Photoluminescence Spectroscopy of QDs

Photoluminescence (PL) spectra of the CdSe/xCdS/2ZnS QDs used for FRET assays were taken with the Horiba Nanolog fluorimeter using a 300/500 grating and collecting at 1024 wavelengths between 550 and 800 nm. Both excitation and emission channels used slit-widths of 2 nm. Collected PL of samples in both hexane and water were graphed and normalized to their emission maxima **(Figure S1)**; PL spectra of uncapped QDs are also shown for comparison. Zinc sulfide (ZnS-) capped QDs show greater size dispersion and full width half max (FWHM) (Figure S1B, S1D). All ZnS capped QDs emit between 610 and 630 nm, making it possible to use the same FRET acceptor for all assays and increasing consistency between experiments.

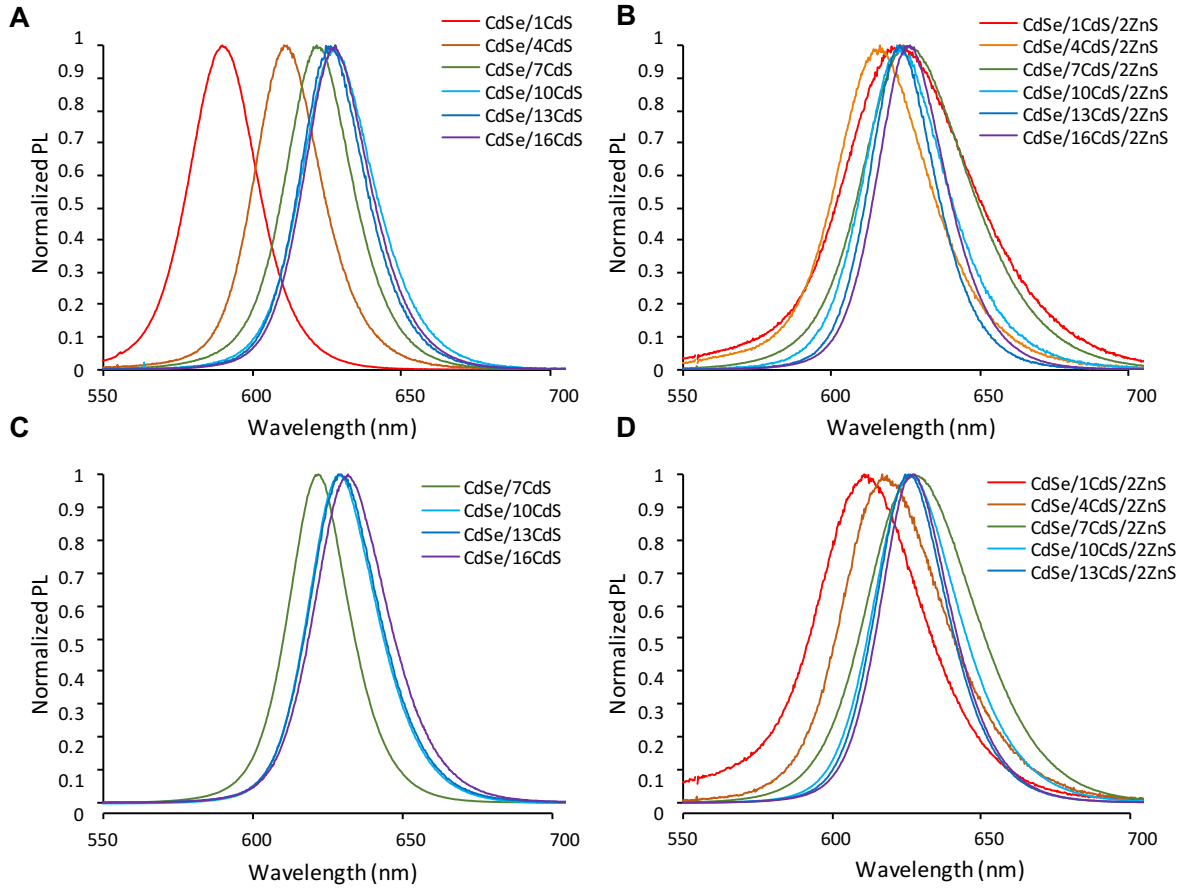

Figure S1: PL spectra taken for (g)QDs without ZnS in (**A**) hexanes and (**C**) CL4/water as well those with ZnS in hexanes (**B**) and water (**D**).

1.2 Lifetime measurements

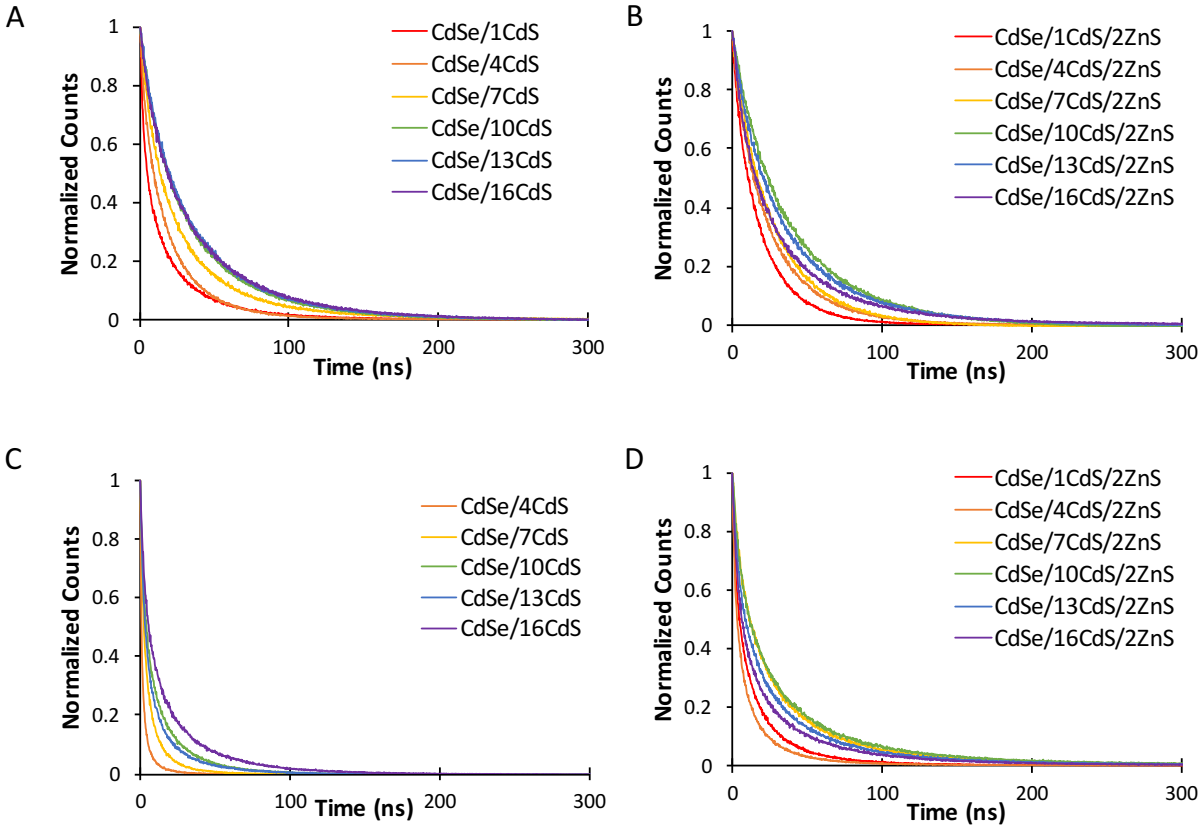

Figure S2: Lifetime measurements for (g)QDs without ZnS in (**A**) hexanes and (**C**) CL4/water as well those with ZnS in hexanes (**B**) and water (**D**).

1.3 Relative Quantum Yield Measurements

QY measurements were taken by graphing a sample's integrated fluorescence intensity as a function of its absorbance and comparing the resulting slope with that of a standard. Absorbance measurements were taken using the CARY 5000 UV/VIS/NIR Spectrophotometer from Varian Inc./Agilent Technologies while fluorescence measurements were taken as previously described. The equation used for calculating relative quantum yield is given as:

$$\Phi_X = \Phi_{ST}\left(\frac{Grad_X}{Grad_{ST}}\right)\left(\frac{\eta_X^2}{\eta_{ST}^2}\right)$$

where Φ is the fluorescence quantum yield, Grad is the slope from the plot of integrated fluorescence intensity vs absorbance, and η is the refractive index of the solvent. Subscripts X and ST denote the test sample and the standard sample, respectively. The standard used for all relative quantum yield measurements was Rhodamine 6G. Rhodamine 6G is known to have a QY of 94%

in ethanol when excited at 488 nm.[1] The QY of the QD samples were taken at 400 nm. To account for the difference in lamp output at 488 and 400 nm, all PL measurements were divided by the lamp intensity.

Table S1: Relative Quantum Yield Values

Sample	Rel. QY in Hexanes (%)	Rel. QY in Water (%)
CdSe/**1**CdS	15.8 ± 1.8	---
CdSe/**1**CdS/2ZnS	19.8 ± 3.8	9.6 ± 0.4
CdSe/**4**CdS	57.2 ± 2.9	---
CdSe/**4**CdS/2ZnS	29.0 ± 2.6	11.9 ± 0.4
CdSe/**7**CdS	60.4 ± 12.8	7.4 ± 1.3
CdSe/**7**CdS/2ZnS	57.4 ± 2.8	37.6 ± 1.1
CdSe/**10**CdS	42.8 ± 2.8	4.9 ± 0.5
CdSe/**10**CdS/2ZnS	55.7 ± 6.8	37.2 ± 1.1
CdSe/**13**CdS	31.3 ± 5.3	1.3 ± 0.7
CdSe/**13**CdS/2ZnS	39.2 ± 4.6	22.1 ± 0.7
CdSe/**16**CdS	19.2 ± 1.2	1.7 ± 1.2
CdSe/**16**CdS/2ZnS	25.9 ± 1.0	14.8 ± 1.0

1.4 Photoluminescence Intensity as a Function of QD Concentration

Differences in PL max intensity from QD brightness based on QY and molar extinction coefficients can be explained by the non-linear nature of PL intensity as a function of QD concentration (**Figure S2**). Because the QDs differ so greatly in size, inner filter effects become apparent in different concentration regimes. Figure S2 shows collected data plotted against a line corresponding to the linear region of the plot. The linear region of each data set was chosen by finding a linear formula that fitted the origin (0,0) and the first data point. The expected value for the concentration of the second data point was then compared against the measured value using a t-test and if $p > 0.05$ then a new fit was formulated to include the second data point. This calculation is carried out until $p < 0.05$ for the next data point. QDs with one, four and seven shells of CdS were found to be linear at concentrations lower than 180, 52, and 205 nM, respectively. The linear range of thicker shelled QDs was found to be lower. QDs with ten, thirteen and sixteen shells of CdS were linear below 22, 23, and 10 nM respectively.

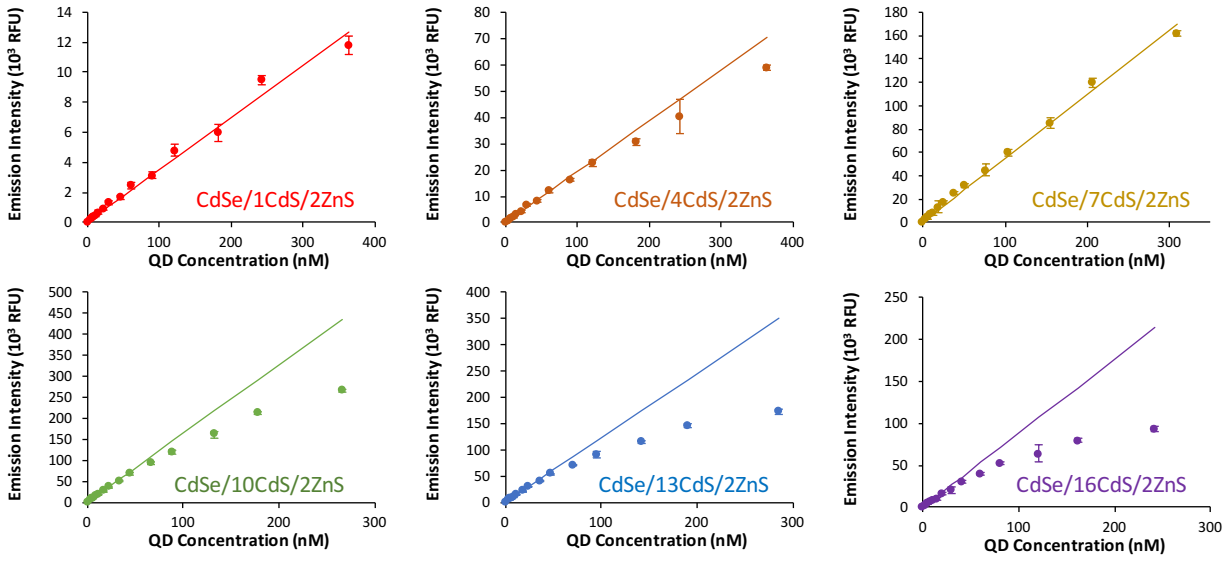

Figure S3: Plots of PL intensity as a function of QD concentration for each QD donor. Measurements were taking in 384 well plates using using 30 µL volumes.

The impact of this inner filter effect was observed when the QD QY measurements were recapitulated at the QD concentrations used in the FRET assays, rather than the very dilute ($OD_{400\ nm}$ < 0.1) concentrations typically recommended for relative QY measurements. At the higher concentrations (ranging from 30 - 50 nM), the procedure used to measure relative quantum yield underestimated the quantum yield significantly (**Figure S3A**). When this is applied to the QD brightness as well (**Figure S3B**), we see that normal assay conditions underutilize the brightness of the thick-shelled QDs. More dilute conditions may see further gains in gQD sensor performance.

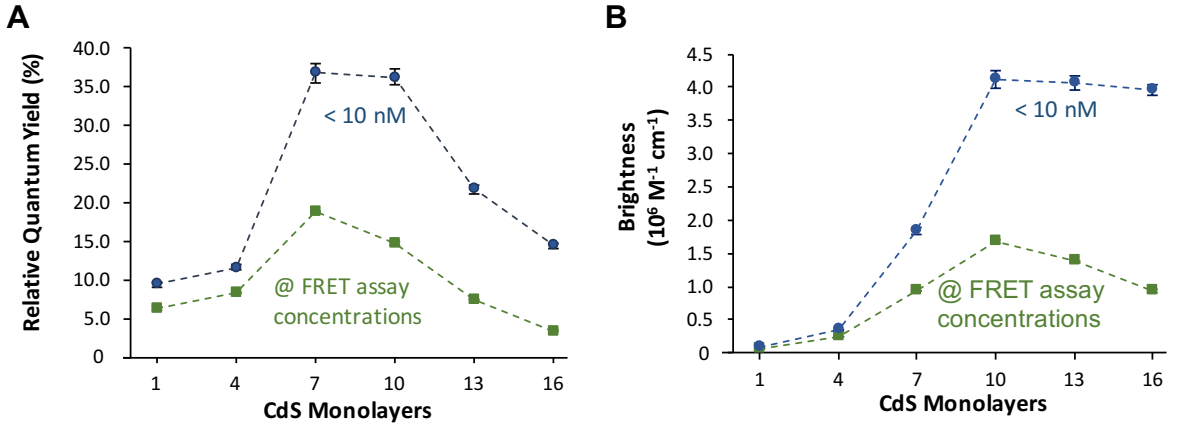

Figure S4: Comparison of (A) shell-thickness dependent relative quantum yield and (B) shell-thickness dependent brightness at very dilute concentrations and typical assay conditions.

2. FRET Assays

Plots of FRET assays using 4, 10 and 16 shelled QD donors are shown in **Figure S4**. The same general trends are seen when using 1, 7, and 13 shelled QD donors.

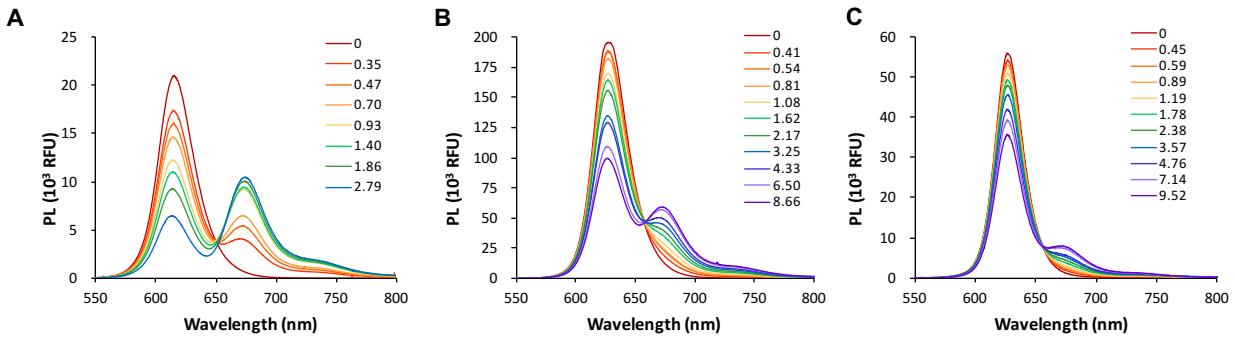

Figure S5: Photoluminescence spectroscopy of FRET between QD donors and increasing numbers of dye-labeled peptides using core/shell/shell nanoparticles donors comprising (**A**) 4, (**B**) 7, or (**C**) 16 CdS monolayers. The legend refers to the number of AF647 acceptor dyes per QD donor. All spectra were background subtracted and averaged across triplicates.

For the CdSe/1CdS/2ZnS and CdSe/4CdS/2ZnS donor, addition of dye in excess of 1.2 or 2.8 acceptors per donor, respectively, results in red-shift and quenching of acceptor emission (**Figure S6**). The same is seen for the CdSe/7CdS/2ZnS donor when adding more than 5.6 acceptors per donor (Figure 3). This behavior is hypothesized to be a result of dye over-crowding and dye-dye energy transfer. Dyes attached the surface of QDs with smaller surface areas will be less spatially separated from each other, resulting in more dye-dye interactions. The limit for oversaturation increases as QD size increases, supporting this explanation.

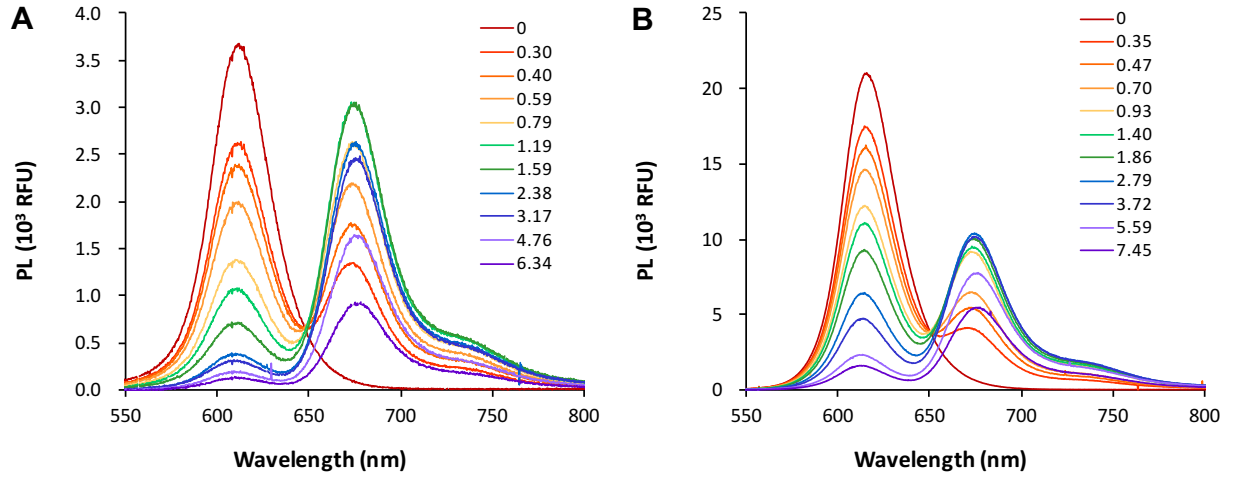

Figure S6: Full spectra of FRET assays using (**A**) CdSe/1CdS/2ZnS and (**B**) CdSe/4CdS/2ZnS QD donors

Plots of F_A/F_D for each QD donor are shown separately in **Figure S7** in order to more easily see the non-linear trend that is apparent in each case. This is not as easily seen visually when plotting all 6 lines together due to the enormous different in range that each QD exhibits.

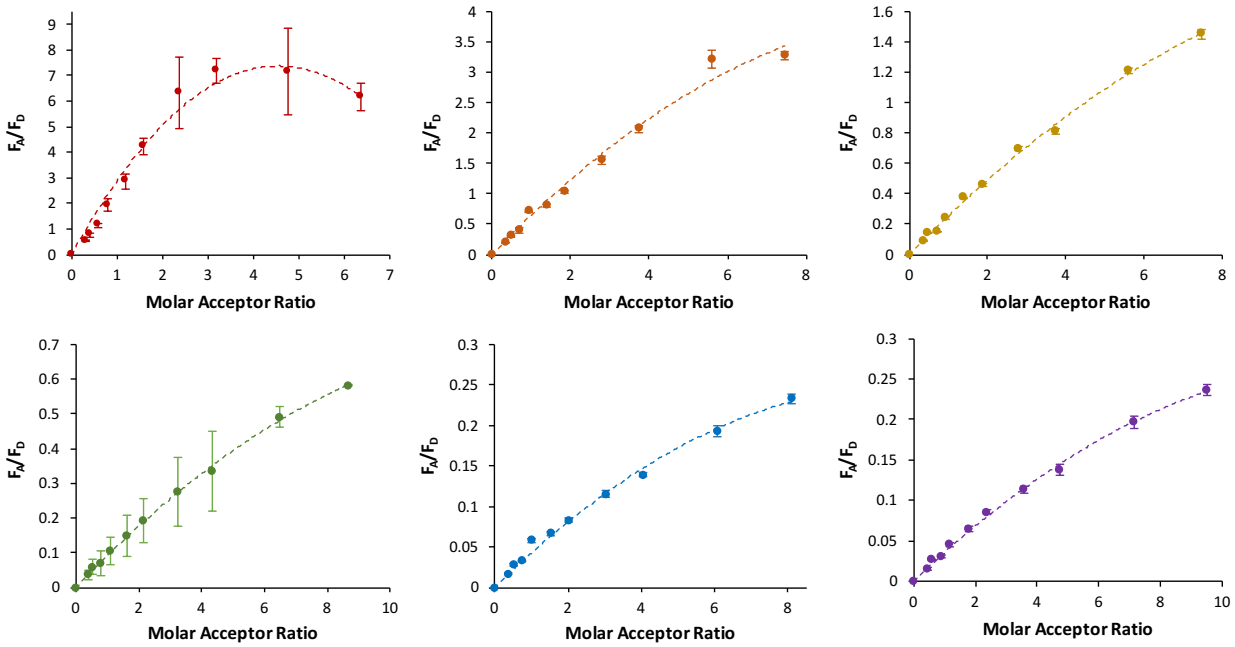

Figure S7: F_A/F_D for a thin (**A**), medium (**B**) and thick (**C**) shelled donor plotted on separate axes.

His-tag binding has been shown to increase QD emission of unevenly coated particles by patching surface defects.[2, 3] Unlabeled peptide was titrated at the same peptide:QD ratios used for the FRET assays to control for His-tag binding effects and this trend was not seen (**Figure S8**).

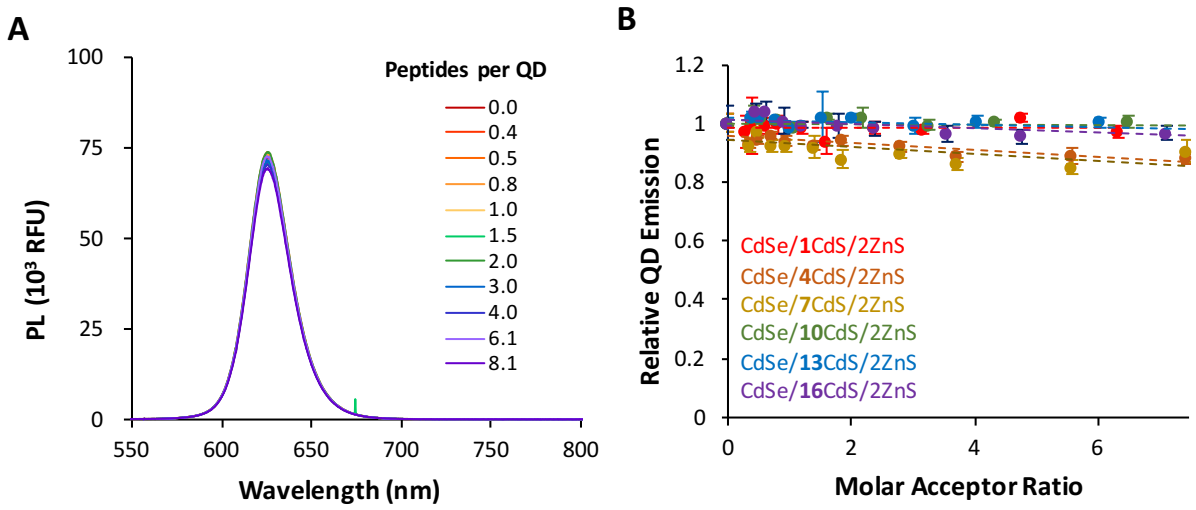

Figure S8: (**A**) Plots of a representative his-tag binding control and the (**B**) change in relative QD emission as additional peptides are added to each QD donor.

Lifetime measurements of the CdSe/xCdS/2ZnS to AF647 are plotted in semi-log scale in **Figure S9**. Each component of the tri-exponential (F980 Software, Edinburg Instruments) used to fit each curve is listed in **Table S2.**

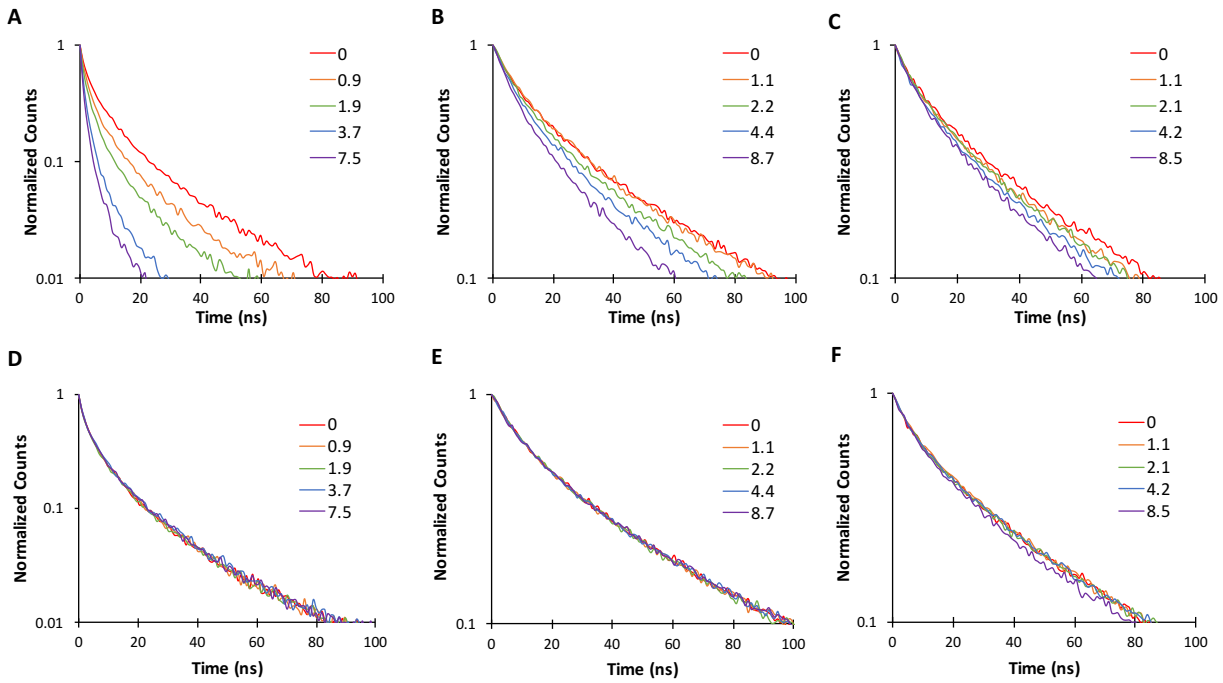

Figure S9: Lifetime plots of the four (**A**), ten (**B**), and sixteen (**C**) shelled donors and their respective controls shown below (**D**, **E**, **F**).

Table S2: FRET Assay Lifetime Fits:

CdSe/4CdS/2ZnS Donor FRET

A:D	A_1	τ_1	A_2	τ_2	A_3	τ_3	τ_{ave}	E_{FRET}
0	3082.74	5.38	2349.58	20.01	153.50	85.25	13.73	0.00
0.9	2996.67	4.05	1781.78	16.55	153.40	68.92	10.58	0.23
1.9	6098.70	2.56	2040.39	11.82	188.87	52.28	5.96	0.57
3.7	2219.76	2.32	807.54	9.89	79.52	46.15	5.41	0.61
7.5	1846.91	1.98	594.68	8.40	62.48	41.89	4.50	0.67

CdSe/10CdS/2ZnS Donor FRET

A:D	A_1	τ_1	A_2	τ_2	A_3	τ_3	τ_{ave}	E_{FRET}
0	3461.95	14.96	3730.01	54.14	465.61	193.71	44.91	0.00
1.1	3837.29	16.50	3473.43	54.84	434.93	191.57	43.52	0.03
2.2	3306.69	12.18	3834.24	43.78	573.24	156.49	38.61	0.14
4.4	3605.82	12.57	3414.94	44.17	422.39	167.36	35.85	0.20

8.7	4181.24	12.71	2654.27	44.30	301.65	167.84	31.01	0.31

CdSe/16CdS/2ZnS Donor FRET

A:D	A_1	τ_1	A_2	τ_2	A_3	τ_3	τ_{ave}	E_{FRET}
0	3271.52	12.57	4150.3	47.23	309.25	185.87	38.11	0.00
1.1	3638.92	12.18	4223.66	44.5	351.38	178.7	35.92	0.06
2.1	3686.82	11.99	4317.54	42.92	338.83	177.65	34.72	0.09
4.2	3727.65	12.19	4018.56	42.14	308.25	181.21	33.60	0.12
8.5	3892.98	11.53	3945.23	38.45	328.79	161.73	30.58	0.20

CdSe/4CdS/2ZnS Non-Binding Control

A:D	A_1	τ_1	A_2	τ_2	A_3	τ_3	τ_{ave}
0	3343.91	5.47	2188.97	20.28	169.84	81.60	13.42
0.9	2923.56	4.94	2518.88	18.28	225.70	71.58	13.52
1.9	2971.04	4.85	2413.72	17.98	263.61	65.21	13.28
3.7	3198.56	5.70	2284.74	20.84	157.08	86.23	14.08
7.5	2806.28	4.63	2659.00	17.51	280.83	64.26	13.50

CdSe/10CdS/2ZnS Non-Binding Control

A:D	A_1	τ_1	A_2	τ_2	A_3	τ_3	τ_{ave}
0	3285.55	14.86	4019.04	51.29	617.86	172.52	45.64
1.1	3522.31	15.63	3901.61	55.22	472.78	197.30	46.07
2.2	3482.55	15.54	3933.23	53.54	510.33	187.18	45.45
4.4	3103.44	13.30	4245.71	50.08	630.89	168.63	45.15
8.7	3141.72	14.71	4130.76	51.89	560.42	179.11	46.08

CdSe/16CdS/2ZnS Non-Binding Control

A:D	A_1	τ_1	A_2	τ_2	A_3	τ_3	τ_{ave}
0	2342.31	12.61	4151.78	45.50	417.60	162.91	41.45
1.1	2897.01	16.15	3696.34	49.82	339.98	177.23	42.00
2.1	2963.10	12.79	4208.00	47.48	353.64	182.91	40.18
4.2	3206.79	15.03	3892.02	49.54	340.94	191.46	41.17
8.5	3080.09	12.57	4102.79	45.24	305.02	188.59	37.64

3. Visual Enzyme Cleavage Assay

Multiple acceptor:donor ratios were tested in the visual assay. Lower numbers of acceptors were sufficient to quench the thin-shelled QDs, but the QD emission was difficult to discern compared to the brighter QDs. For the medium- and thick-shelled gQDs, visible quenching due to the binding of the dye-labeled peptide was difficult to visualize by eye.

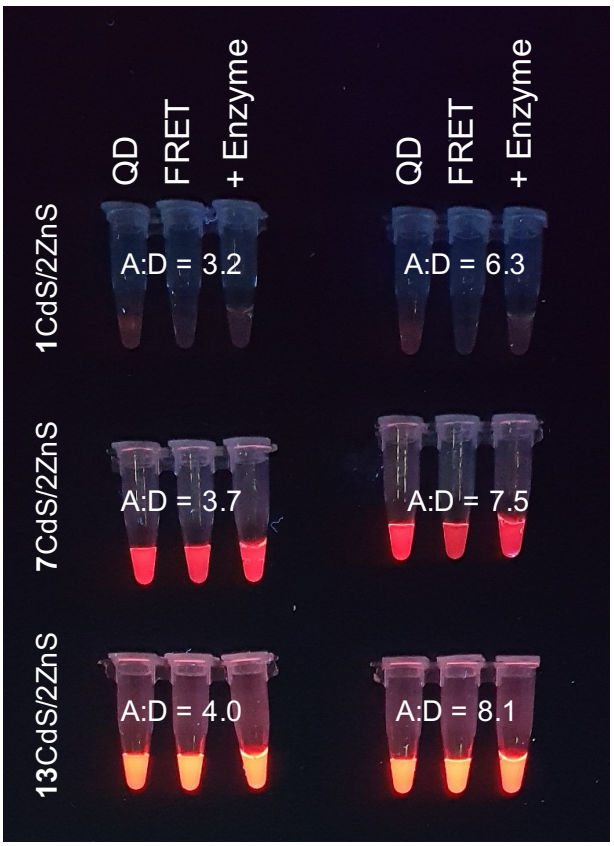

Figure S10: Comparison of visual sensors for different QD donors at the QD concentrations used in Figure 3 and acceptor/donor ratios as noted. Top to bottom: thin, medium and thick shelled donors. Left to right: QD only, QD A647 FRET quenching, QD + A647 + enzyme.

References

1. M. Fischer and J. Georges, *Chemical Physics Letters*, 1996, **260**, 115-118.
2. A. M. Dennis, D. C. Sotto, B. C. Mei, I. L. Medintz, H. Mattoussi and G. Bao, *Bioconjug Chem*, 2010, **21**, 1160-1170.
3. A. R. Clapp, I. L. Medintz, J. M. Mauro, B. R. Fisher, M. G. Bawendi and H. Mattoussi, *Journal of the American Chemical Society*, 2004, **126**, 301.